Pakistan Veterinary Journal

ISSN: 0253-8318 (PRINT), 2074-7764 (ONLINE)
DOI: 10.29261/pakvetj/2026.058

RESEARCH ARTICLE

Chebulagic Acid Ameliorates LPS-Induced Endometritis by Moderating HIF-1α/P53 Signaling Pathways in Dairy Cows

Ruifeng Gao[1†], Fuxiang Bao[1†], Ying Yang[1], Xinyu Ren[1], Feifan Zhao[1], Hind Althagafi[2], Eman A. Al-Shahari[3], Zhiguo Gong[1*] and Zhiheng Zhang[1*]

[1]College of Veterinary Medicine, Inner Mongolia Agricultural University, Hohhot, 010018, China; [2]Department of Biology, College of Science, Princess Nourah bint Abdulrahman University, P.O. Box 84428, Riyadh 11671, Saudi Arabia; [3]Health Specialties, Basic Sciences and Their Applications Unit, Applied College at Muhayil Asir, King Khalid University, Abha, Saudi Arabia. † This author made an equal contribution to this work.
*Corresponding author: 15648194032@163.com (ZG); zzh449756020@163.com (ZZ)

ARTICLE HISTORY (26-045)

Received: January 18, 2026
Revised: February 20, 2026
Accepted: February 23, 2026
Published online: March 05, 2026

Key words:
Dairy cow
Endometritis
Chebulagic Acid
HIF-1α/p53 pathway

ABSTRACT

Endometritis is a leading cause of reproductive failure in dairy cows, which is unfavorable for livestock production and the agricultural industry. Moreover, the widespread presence of antibiotic residues in milk after treatment raises serious public health concerns. The present study focuses on the protective interventions of Chebulagic Acid (CA) on lipopolysaccharide (LPS)-induced endometritis in dairy cow endometrium. The endometrial tissues were incubated with LPS and divided into the following five groups: control, LPS, LPS+CA, LPS+CA, and LPS+CA. The results showed in pathological histological changes and pro-inflammatory cytokines indicated the anti-inflammatory effect of CA on endometrial tissue. Through network pharmacology and molecular dockings, IL-1β, BCL2, TP53, TNF, and HIF-1A were identified as central therapeutic targets of CA. CA effectively downregulated the expression of HIF-1A and TP53. CA also suppressed the levels of COX-2, IL-1β, MMP-2, IL-6, iNOS, TNF-α, ALOX-15, and HMGB-1, thereby alleviating inflammation and safeguarding endometrial tissue in cases of endometritis. The results suggest that CA mitigates the synthesis of pro-inflammatory factors and protects the endometrium from inflammatory damage in dairy cows through the HIF-1α/p53 pathway.

To Cite This Article: Gao R, Bao F, Yang Y, Ren X, Zhao F, Althagafi H, Al-Shahari EA, Gong Z and Zhang Z, 2026. Chebulagic acid ameliorates LPS-induced endometritis by moderating hif-1α/p53 signaling pathways in dairy cows. Pak Vet J, 46(3): 691-700. http://dx.doi.org/10.29261/pakvetj/2026.058

INTRODUCTION

Endometritis, a prevalent uterine disorder associated with reproductive failure (Purba *et al.*, 2021), is a significant contributor to premature culling of dairy cows and substantial socioeconomic burdens (Zhao *et al.*, 2024; Liu *et al.*, 2025). The pathogenesis of endometritis is primarily attributed to microbial infections, with *Escherichia coli* (*E. coli*) being the predominant causative agent. *E. coli* induces endometrial inflammation and histological damage through the release of lipopolysaccharide (LPS) (Jiang *et al.,* 2021; Talib *et al.,* 2025). Although antibiotic therapy remains the standard clinical intervention, the detection of antibiotic residues in milk poses notable public health risks (Cao *et al.*, 2024). As a result, effective alternative therapies are urgently needed.

Under conditions of acute hypoxia, the expression of numerous downstream genes is regulated by hypoxia-inducible factor 1 (HIF-1), which helps mitigate cellular damage caused by hypoxic stress (Wu *et al.*, 2018; Liang *et al.*, 2023; Cao *et al.*, 2024). HIF-1α, a key subunit of HIF-1, plays a critical role in pathways regulating cellular metabolism and significantly influences immune cell function (Corcoran and O'Neill, 2016). Recent findings suggest that HIF-1α contributes to the pathogenesis of endometritis, as it is upregulated in uterine tissues during endometrial inflammation; conversely, suppression of inflammation reduces HIF-1α levels (Cao *et al.*, 2024). P53 plays a pivotal role in cell cycle regulation and functions as a key mediator of growth arrest, senescence, and apoptosis in cellular stress (Heckl *et al.*, 2018). Post-translational modifications of p53 have been demonstrated to initiate and modulate inflammatory signaling pathways. Therefore, the potential involvement of p HIF-1α/53 in the pathogenesis of endometritis merits further investigation.

Chebulagic acid (CA), a 691 ydrolysable tannin, constitutes a key active ingredient in Garidi-13, a

traditional Mongolian formulation used for thrombosis prevention (Liu *et al.*, 2015). CA exhibits anti-inflammatory and antitumor properties. It has been demonstrated to exert anti-inflammatory effects in LPS-stimulated RAW 264.7 macrophages and endothelial cells. (Kumar *et al.*, 2014; Liu *et al.*, 2015; Ekambaram *et al.*, 2022). Recently, CA was reported to attenuate inflammation in murine models of LPS-induced endometritis (Liu *et al.*, 2025). Nevertheless, current research remains limited, and few studies have systematically examined the protective or therapeutic potential of CA in bovine endometritis.

In this study, we systematically assessed the anti-inflammatory effects of CA in a model of LPS-induced endometritis. Key molecular targets were identified that combined network pharmacology, molecular docking, and molecular dynamics (MD) simulations, and the underlying mechanisms were experimentally validated.

MATERIALS AND METHODS

In-vitro model construction of endometritis: Endometrial tissue was collected from healthy Holstein dairy cows at a local abattoir. The fresh tissue was washed twice with PBS at 4°C under aseptic conditions. The tissue was thoroughly minced and incubated in DMEM/F12 (Gibco, China) supplemented with 20% fetal bovine serum (FBS, Ex-Cell Biology, Inc., China) and 2% penicillin-streptomycin.

The tissues were treated with 1μg/mL LPS (InvivoGen, USA) for 1h, followed by treatment with CA at concentrations of 12.5, 25, 50, and 100μg/mL for 6, 12, and 24h. The LPS concentration was selected based on established protocols using endometrial tissues in prior studies (Peng-Fei *et al.*, 2021). Endometrial tissues and supernatants were collected for subsequent analyses.

HE staining: Scaffolds for histology were fixed using 4% PFA. Specimens were dehydrated in graded alcohol dilutions and embedded in paraffin. Sections were sliced into 5μm. These sections were subjected to HE staining, and pathological damage was assessed using a microscope.

Measurement of pro-inflammatory cytokine levels: The levels of IL-1β, IL-6, and TNF-α in uterine tissues were measured using commercial ELISA kits (CSB-E12986B, CUSABIO for IL-1β; DY8190, R&D Systems for IL-6; and DY2279, R&D Systems for TNF-α). Tissues were collected and homogenized, with the resulting extracts then analyzed. Absorbance was read at 450nm using a microplate reader. (BioTek, USA).

Screening of CA and endometritis targets: The PubChem ID, 2D structure, and isomeric SMILES of CA were retrieved from PubChem. Potential targets of CA were predicted using the isomeric SMILES through four databases: SwissTargetPrediction, ChEMBL, PharmMapper, and the Comparative Toxicogenomics Database. The predicted target lists were then integrated by merging results and removing duplicates, yielding a set of potential CA targets.

Dairy cows' endometritis-related targets were extracted from two disease databases: a search was conducted on the Comparative Toxicogenomics Database (CTD) and GeneCards, using the term "endometritis" as a search term. The screening criteria established were as follows: firstly, a relevance score of 2 or higher in the CTD database, and secondly, a relevance score of 0.2 or higher in the GeneCards database. The experimental dataset was annotated using the UniProt database to ensure uniformity in target nomenclature throughout the study. The associated objectives from the two databases were subsequently integrated, and redundant objectives were removed to produce a definitive list. CA-target-endometritis-pathway networks were visualized using Cytoscape 3.9.

Identification of Targets and Establishment of the PPI Network: Overlapping genes between CA-related targets and bovine endometritis-associated genes were analyzed to identify potential therapeutic targets, with a Venn diagram used to show the intersection.

These shared targets were then imported into the STRING database to construct a PPI (Protein-Protein Interaction) network for further analysis (Szklarczyk *et al.*, 2023). The screening criteria entailed the selection of Bos taurus, with a medium confidence level (0.400 or higher), while ensuring the concealment of disconnected nodes, thereby facilitating the construction of the PPI network. The identification of the core targets was achieved by employing six topological parameters within the network, namely Degree, Betweenness, Radiality, MCC, MNC, and EPC. This facilitated the determination of the top 16 targets.

GO and KEGG analysis: Functional enrichment analysis of the key genes was performed using the DAVID Bioinformatics Resources, integrating Gene Ontology (GO) and Kyoto Encyclopedia of Genes and Genomes (KEGG) databases to systematically characterize their biological functions and associated pathways. Concurrently, KEGG pathway enrichment analysis identified key pathways associated with CA's anti-endometritis mechanism. The results of both GO and KEGG analysis were then subjected to visualization through the utilization.

Molecular docking of CA and key targets: The 3D structure models of the proteins TNF (PDB: 2AZ5), TP53 (PDB: 2J21), IL-1β (PDB: 2E7A), and BCL2 (PDB: 7Z4T) were available in the UniProt database (https://www.uniprot.org). The Schrödinger2021 Maestro12.8 program was used for molecular docking, and PyMOL 3.1.3 was used to analyze and visualize the results. The protein import process into PyMOL involved removing the original ligand and water molecules. The proteins were then imported into AutodockTools (v1.5.7) for preprocessing, including the addition of hydrogen atoms, calculation and assignment of charges, and definition of atom types. The docking box was centered on the original ligand when present; otherwise, the binding site was defined based on the region surrounding previously reported key amino acid residues.

MD Simulation: Molecular dynamics (MD) simulations of CA and its core targets were conducted using GROMACS to

validate the predictions derived from network pharmacology. Force field parameters were generated with the pdb2gmx tool and supplemented with data from AutoFF (Jo *et al.*, 2008). The amber14sb force field was assigned to the receptor protein, while CGenff was applied to the ligand. The system was solvated in a 1nM cubic box of TIP3P water molecules neutralized by adding counterions via the gmx genion module, and treated for long-range electrostatic interactions using the Particle Mesh Ewald (PME) method with a cutoff of 1nM (Harrach and Drossel, 2014). Bonds involving hydrogen atoms were constrained using the SHAKE algorithm, and equations of motion were integrated using the Verlet leapfrog integrator with a time step of 1 fs. Energy minimization consisted of 3,000 steps of steepest-descent followed by 2,000 steps of conjugate-gradient optimization, implemented in a stepwise manner: initially with the solute restrained and the solvent minimized, then with counterions restrained, and finally with no restraints applied to the entire system. The production simulation was carried out under NPT ensemble conditions (310 K, constant pressure) for a total duration of 100ns.

Real-time PCR: Total RNA was extracted, reverse transcribed, and quantified using a commercial kit, premix, and SYBR Green Master Mix. The PCR reaction consisted of 40 cycles of 15s at 94°C and 30s at 60°C, with an initial 10min hot start at 94°C. Amplification was carried out using the ABI QuantStudio 7 (Applied Biosystems, Waltham, MA, USA). The primers used were manufactured by Invitrogen (Carlsbad, CA, USA), and their sequences are listed in Table 1. The mRNA expression was then calculated using the 2-$^{\triangle\triangle}$Ct method.

Table 1: The information on the primer sequence is designed.

Gene	Forward	Reverse
COX-2	*GGTGCCTGGTCTGATGATGT*	*GATTAGCCTGCTTGTCTGGAAC*
MMP-2	*GGCATCTCTCAGATCCGTGG*	*TGTGGGTCTTCGTACACAGC*
TP53	*TGAACCGCCGACCTATCCTTA*	*GGCACAAACACGAACCTCAAA*
HIF-1A	*GCCGGGGGAGAACTATGAAC*	*ACAAATCAGCACCAAGCACG*
ALOX15	*CTTTCCACTGTCCACACCCA*	*GATCAAGGAGGAAGGACGGG*
HMGB-1	*AATCAAGGCGAACATCCTG*	*ATCCGCAGCAGTGTTATTCC*
iNOS	*AGCGGAGTGACTTTCCAAGA*	*TTTTGGGGTTCATGATGGAT*
β-actin	*CCAAGGCCAACCGTGAGAAGAT*	*CCACGTTCCGTGAGGATCTTCA*

Western Blot analysis: Total proteins were extracted using T-PER Tissue Protein Extraction Reagent, and protein concentrations were quantified. Equal amounts of protein (20μG) were separated and transferred by SDS-PAGE and PVDF membranes for immunoblotting analysis. The membranes were blocked with 3% BSA for 4h and then incubated overnight at 4°C with primary antibodies against COX-2 (AF7003, 1:1000), HIF-1A (BF0593, 1:1000), MMP-2 (AF5330, 1:1000), p53 (BF8013, 1:1000), ALOX15(DF13494, 1:1000), HMGB-1 (AF7020, 1:1000), iNOS (AF0199, 1:1000) and GAPDH (AF7021, 1:1000). The bands were incubated at room temperature with a HRP - labeled secondary antibody. All antibodies from Affinity Biosciences (Cincinnati, OH, USA). The blots were detected using an ECL kit, and protein band intensities were quantified with ImageJ.

Statistical analysis: SPSS version 25.0 and GraphPad Prism version 9 (USA) for the statistical analysis were utilized for the analysis of the data. Data are expressed as mean ± standard deviation (SD). Group comparisons were performed using one-way ANOVA and the two-tailed Student's t-test. A statistical significance level of $P<0.05$ was applied to all comparisons.

RESULTS

CA alleviated inflammation in LPS-induced dairy cow endometrial tissues: HE staining showed that endometrial tissue in the control group had a healthy morphology, with intact architecture and ciliated epithelial cells. Longitudinal sections revealed a continuous, uniformly organized luminal epithelium and well-preserved glands clearly visible in the stroma (Fig. 1A). In contrast, bovine endometrial tissues exposed to LPS exhibited progressive histological damage, including reduced visibility of endometrial glands, loss of both luminal and glandular epithelial cells, and disruption of the vascular endothelium (Fig. 1B). The compromised tissue architecture indicated significant endometrial injury. In the LPS+CA group, notable improvements were observed compared to the LPS group, including reduced epithelial cell detachment, better preservation of glandular and vascular structures, decreased inflammatory cell infiltration, and absence of significant necrosis or hemorrhage. These findings suggest that CA mitigates LPS-induced endometrial damage, demonstrating its protective effect on endometrial tissue in dairy cows (Fig. 1C-F).

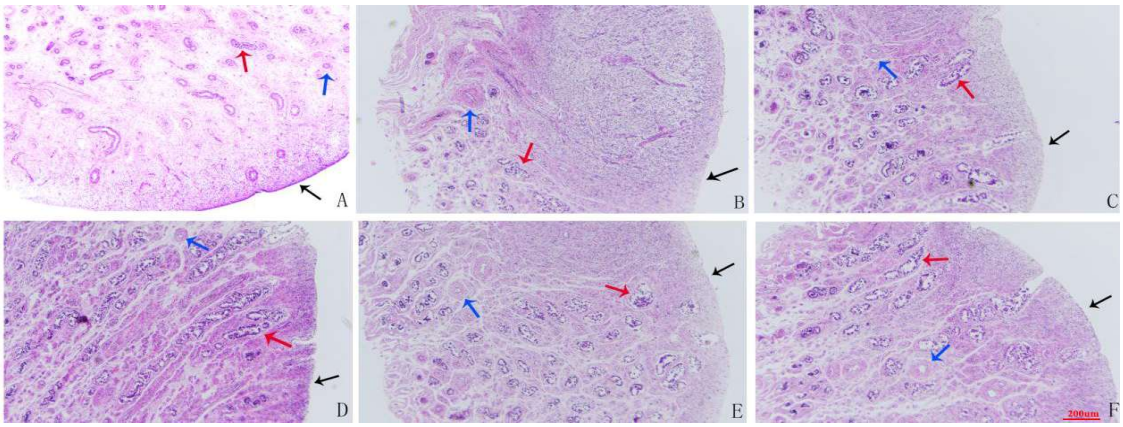

Fig. 1: The morphology of endometrial tissue in LPS-stimulated dairy cows was examined for the effect of CA through HE staining. A. group CON, B. LPS, C–F were co-treated with LPS and increasing concentrations of CA (12.5, 25, 50, and 100 μg/mL) to study the dose-dependent effect. Black arrows indicate endometrial epithelial cells, the red arrows indicate glands, and the blue arrows indicate blood vessels (magnification ×200).

ELISA analysis demonstrated that LPS stimulation markedly upregulated the levels of pro-inflammatory cytokines IL-6, TNF-α, and IL-1β (Fig. 2A–C). IL-6 and IL-1β levels were significantly elevated at 6, 12, and 24 hours (Fig. 2A, C), whereas TNF-α showed a significant increase at 12 hours (P<0.0001) and remained elevated at 24 hours (P<0.01; Fig. 2B). In contrast, CA treatment effectively suppressed the LPS-induced expression of all three cytokines. Notably, 25 and 50μg/mL CA significantly inhibited IL-6, TNF-α, and IL-1β (P<0.05) at 6, 12, and 24 hours, indicating a consistent anti-inflammatory effect over time. These findings strongly suggest that CA attenuates LPS-induced inflammation in endometrial tissue.

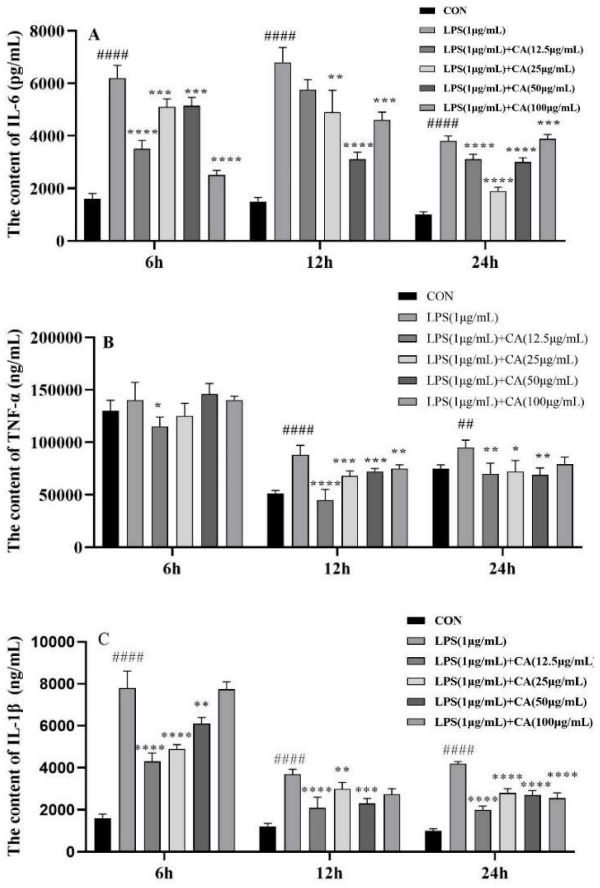

Fig. 2: The effect of CA on LPS-induced inflammatory responses in bovine endometrial tissue. (A) IL-6, (B) TNF-α, (C) IL-1β. * and # denote statistical significance compared to the Con and LPS groups, respectively; *# indicates P<0.05, **## indicates P<0.01, ***### indicates P<0.001, and ****#### indicates P<0.0001.

Network pharmacology reveals molecular mechanisms of CA in dairy cow endometritis

Core targets and signaling pathways: A total of 363 potential targets for CA were identified, including 8 from CTD, 215 from ChEMBL, 123 from PharmMapper, and 100 from SwissTargetPrediction. 2270 endometritis targets were collected, and 76 of these intersected with potential CA targets, as exhibited in Fig. 3A, B. Subsequently, the PPI network was established regarding the overlap between disease-related pathways and drug targets through the utilization of the STRING database (Fig. 3C). Six algorithms yielded 16 overlapping hub gene targets (Fig. 3D), namely IL-1β, SR2, PPARγ, ERBB2, BCL2, TGFB1, TP53, SRC, TNF, APP, IGF1R, STAT1, HIF-1A, MMP2, PRKACA, and HDAC1. Functional enrichment analysis of the 76 targets was performed using GO and KEGG. As illustrated in the BP category, the main enrichment was gland development, response to oxygen levels, and reactive oxygen species metabolic process (Fig. 3E, F). In the MF category, the primary enrichments were transcription coregulator binding, oxidoreductase activity, and aromatase activity. Within the CC analysis, the main enriched terms were membrane raft, membrane microdomain, and plasma membrane raft. Furthermore, most enriched pathways included P53, NF-kappa B, HIF-1, and the MAPK signaling pathway following the HUB targets (Fig. 3G, H). The potential therapeutic targets were subsequently integrated to establish a comprehensive CA-target-pathway-endometritis interaction network (Fig. 3I).

Molecular docking verification of CA and endometritis: Hub targets were validated through molecular docking. The binding energies derived from molecular docking are presented in Fig. 4A. Based on these findings, we hypothesize that the anti-inflammatory effects of CA are mediated by key targets, including IL-1β, TNF, BCL2, and TP53. Three-dimensional visualizations of the molecular docking interactions between CA and the target proteins IL-1β, TNF, BCL2, and TP53 (exhibiting the strongest binding affinities) were generated, confirming stable ligand-protein complexes (Fig. 4B-E).

MD Simulations: MD simulations were performed on four protein-ligand complexes to assess the structural stability. IL-1β-CA, TNF-CA, BCL2-CA, and TP53-CA. RMSD values reflect the stability of CA's binding conformation to the target site, with lower scores indicating greater stability. As illustrated in Fig. 5A, the IL-1β-CA complex reached equilibrium after 90ns, with fluctuations stabilizing around 1.6Å. The BCL2-CA complex achieved equilibrium after 5 ns, exhibiting fluctuations around 2.9Å. Meanwhile, the TNF-CA complex reached equilibrium after 70ns, with fluctuations stabilizing at approximately 2.4Å. The TP53-Chebulagic acid complex displayed stable fluctuations between 5 and 30ns, followed by minor fluctuations after 30ns, with overall fluctuations remaining below 5.1Å. These findings demonstrate that CA binds stably to the target proteins IL-1β, BCL2, TNF, and TP53.

Rg represents the mass-weighted average radius of gyration of the system during the simulation and is widely used to evaluate structural compactness and stability in protein–ligand interactions. A greater change in Rg indicates increased system expansion. The complexes of IL-1β–CA, BCL2–CA, TNF–CA, and TP53–CA exhibited only minor fluctuations in Rg throughout the simulation, suggesting that these small–molecule–protein complexes underwent gradual conformational adjustments without significant structural disruption (Fig. 5B). SASA is a key metric for assessing the solvent-accessible surface area of proteins. The SASA values for the target–ligand complexes were calculated (Fig. 5C). Our results show that the complexes formed by IL-1β with CA, BCL2 with CA, TNF with CA, and TP53 with CA displayed minimal fluctuations, indicating stable intermolecular interactions.

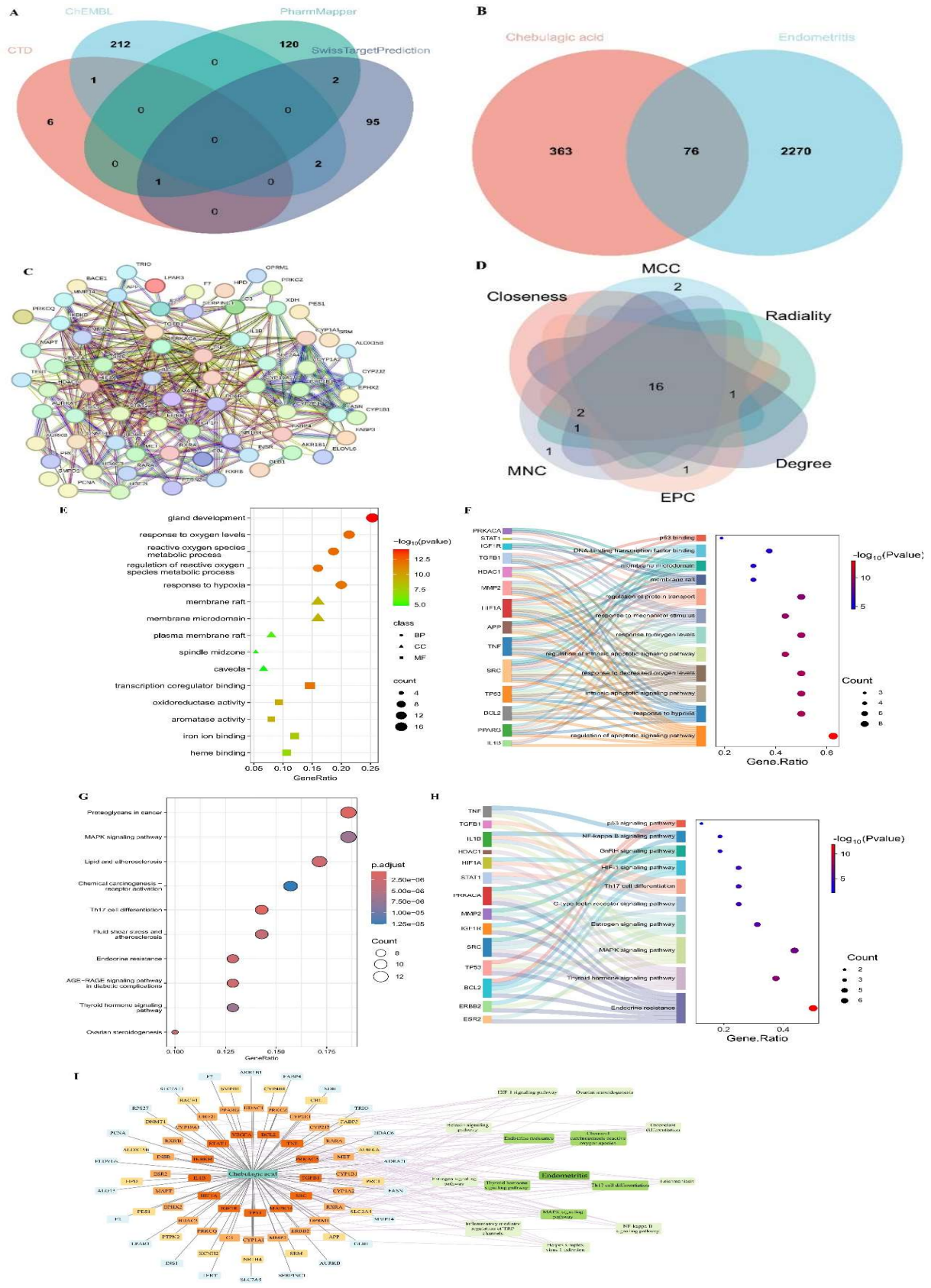

Fig. 3: PPI analysis of CA for the management of endometritis in dairy cows. (A) screening of the CA targets; (B) A Venn diagram (CA and endometritis targets). (C) CA -PPI network; (D) Cytoscape Hubba six latitude screening HUB genes. MCC, maximum clique centrality; EPC, Edge Percolated Component; MNC, Neighborhood Component Centrality; (E) GO enrichment analysis; (F) Sankey dot plot of GO enrichment analyses; (G) KEGG enrichment analysis; (H) Sankey dot plot of KEGG pathways; (I) CA-target-pathway- endometritis. Core nodes of the network were identified as targets with high Closeness, MCC, EPC, NMC, Radiality, and Degree greater than the median.

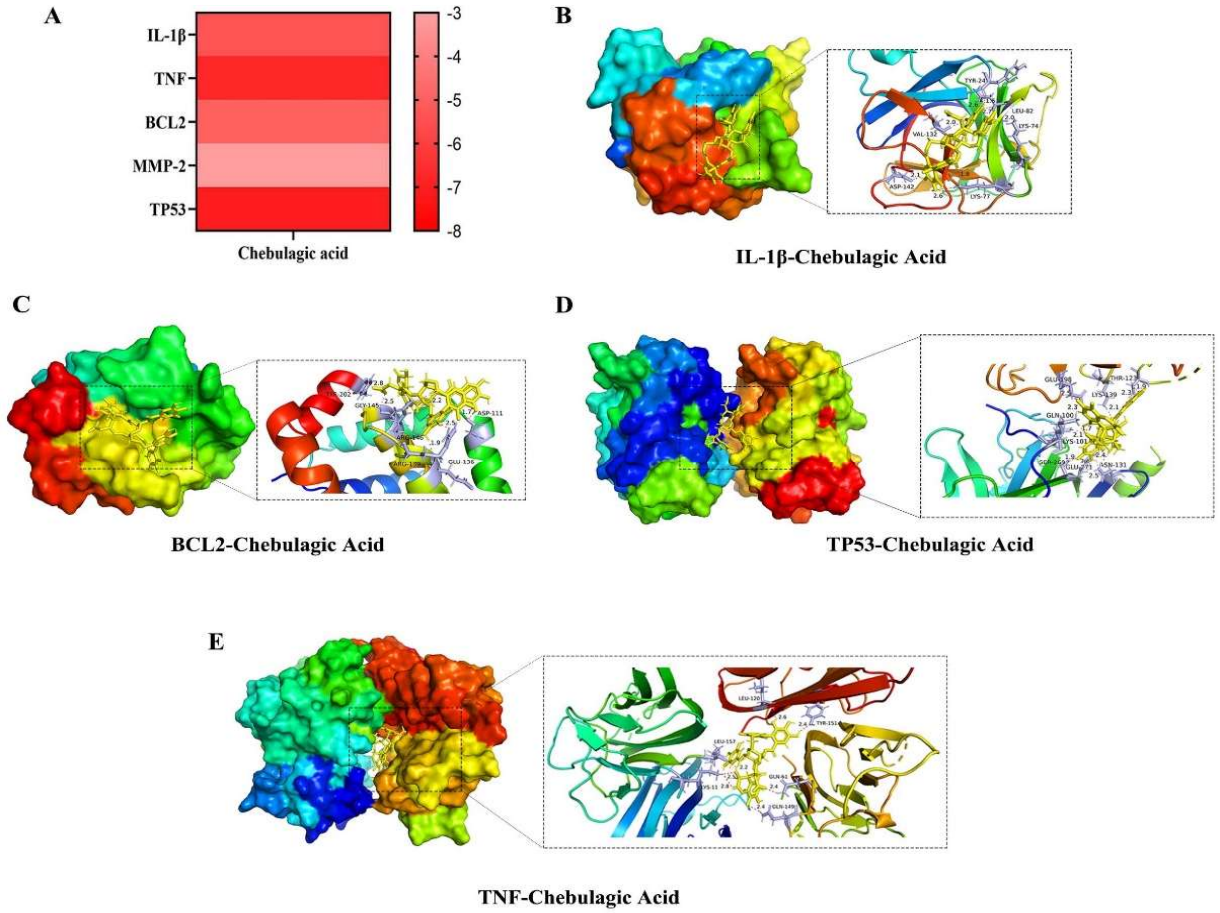

Fig. 4: Molecular docking. (A) Molecular docking scores indicated a higher binding capacity; the deeper the red color, the stronger the binding energy; (B) IL-1β-CA; (C) TNF-CA; (D) TP53-CA; (E) BCL2-CA.

Fig. 5D illustrates the dynamic interactions between CA and its target proteins throughout the simulation. The IL-1β-CA complex maintained an average of approximately two hydrogen bonds, indicating a stable but modest interaction. BCL2–CA exhibited fluctuations between 0 and 11 hydrogen bonds, with a mean of seven. TNF-CA displayed a range of 0 to 13, most frequently sustaining around 10 hydrogen bonds. TP53-CA showed a similar profile, ranging from 0 to 12 and averaging approximately seven. These findings demonstrate that CA consistently forms hydrogen bonds with all four target proteins, supporting its role in stabilizing protein-ligand complexes. Furthermore, RMSF analysis revealed that all complexes exhibited low fluctuation amplitudes, predominantly below 4Å (Fig. 5E), which reflects limited residue mobility and enhanced structural stability upon CA binding. Taken together, these results strongly support that CA effectively engages with IL-1β, BCL2, TNF, and TP53, functioning as a stable molecular modulator.

CA-regulated HIF-1α/p53 signaling to reduce inflammatory factors in endometrial tissues of dairy cows: As shown in Fig. 6, LPS treatment significantly upregulated the mRNA expression of pro-inflammatory markers (COX-2, iNOS, ALOX-15, MMP-2, and HMGB-1) compared to the control group. CA administration effectively reduced their mRNA levels in a time-dependent manner at 6, 9, and 12h. Notably, treatment with 25μg/mL and 50μg/mL CA led to significant suppression of COX-2, iNOS, ALOX-15, MMP-2, and HMGB-1($P<0.05$) at 9 and 12h relative to the LPS group (Fig. 6A-E). These findings support that CA attenuates LPS-induced endometritis by downregulating pro-inflammatory mRNA expression. Furthermore, LPS significantly increased p53 and HIF-1α mRNA levels compared to control, whereas CA treatment markedly downregulated both targets at 6, 9, and 12h ($P<0.05$; Fig. 6F-G).

We investigated the protein levels of key inflammatory mediators in LPS-induced endometrial tissues following 12 h CA treatment (Fig. 7A). As expected, LPS significantly upregulated all target proteins (COX-2, iNOS, ALOX-15, MMP-2, and HMGB-1) compared to the Con group. Specifically, treatment with CA at concentrations of 12.5, 25, 50 and 100μg/mL inhibited COX-2 expression compared with LPS treatment (Fig. 7B). CA administration (25 and 50μg/mL) was also effective in decreasing LPS-induced higher expression of MMP-2 ($P<0.05$; Fig. 7C). Furthermore, 12.5, 25 and 50μg/mL of CA remarkably decreased LPS-induced production of iNOS, while 100μg/mL significantly increased the protein expression ($P<0.0001$; Fig.8D). In addition, CA (50 and 100μg/mL) treatment downregulated P53 expression, and HIF-1α and ALOX5 expression were inhibited by CA compared to the LPS group ($P<0.05$; Fig. 7D-G). Lastly, 12.5, 25, and 50μg/mL of CA led to a reduction of HMGB-1, which was increased by LPS induction ($P<0.01$; Fig. 7H).

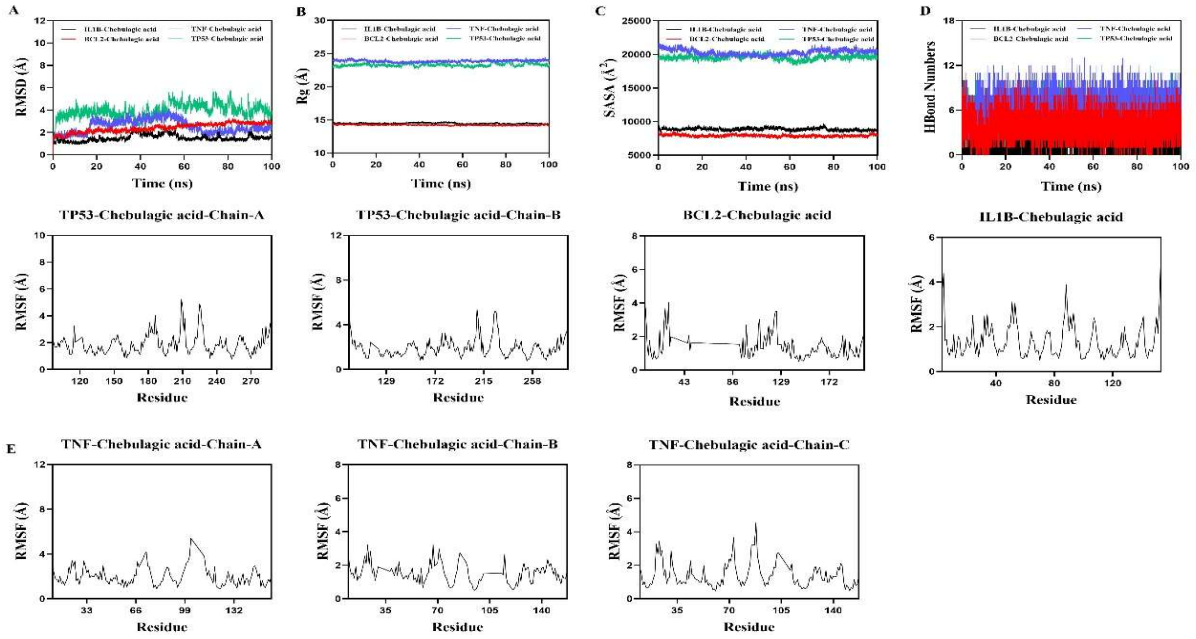

Fig. 5: MD simulation analysis of complex dynamics. (A) MD simulations exceeding 100 ns were employed to investigate the dynamic behavior of complex systems, yielding RMSD trajectories for the IL-1β-CA, TNF-CA, TP53-CA, and BCL2-CA complexes. (B) Rg was calculated throughout the MD simulations to assess structural compactness, with Rg profiles generated for each of the IL-1β-CA, TNF-CA, TP53-CA, and BCL2-CA complexes. (C) SASA plots were computed for the IL-1β-CA, TNF-CA, TP53-CA, and BCL2-CA complexes as part of the MD analysis. (D) Hydrogen bond formation was monitored over the course of the MD simulations, and the average number of hydrogen bonds was recorded for each complex: IL-1β-CA, TNF-CA, TP53-CA, and BCL2-CA. (E) Residue-level flexibility was analyzed by computing root mean square fluctuation (RMSF) profiles for the IL-1β-CA, TNF-CA, TP53-CA, and BCL2-CA complexes during the MD simulation runs.

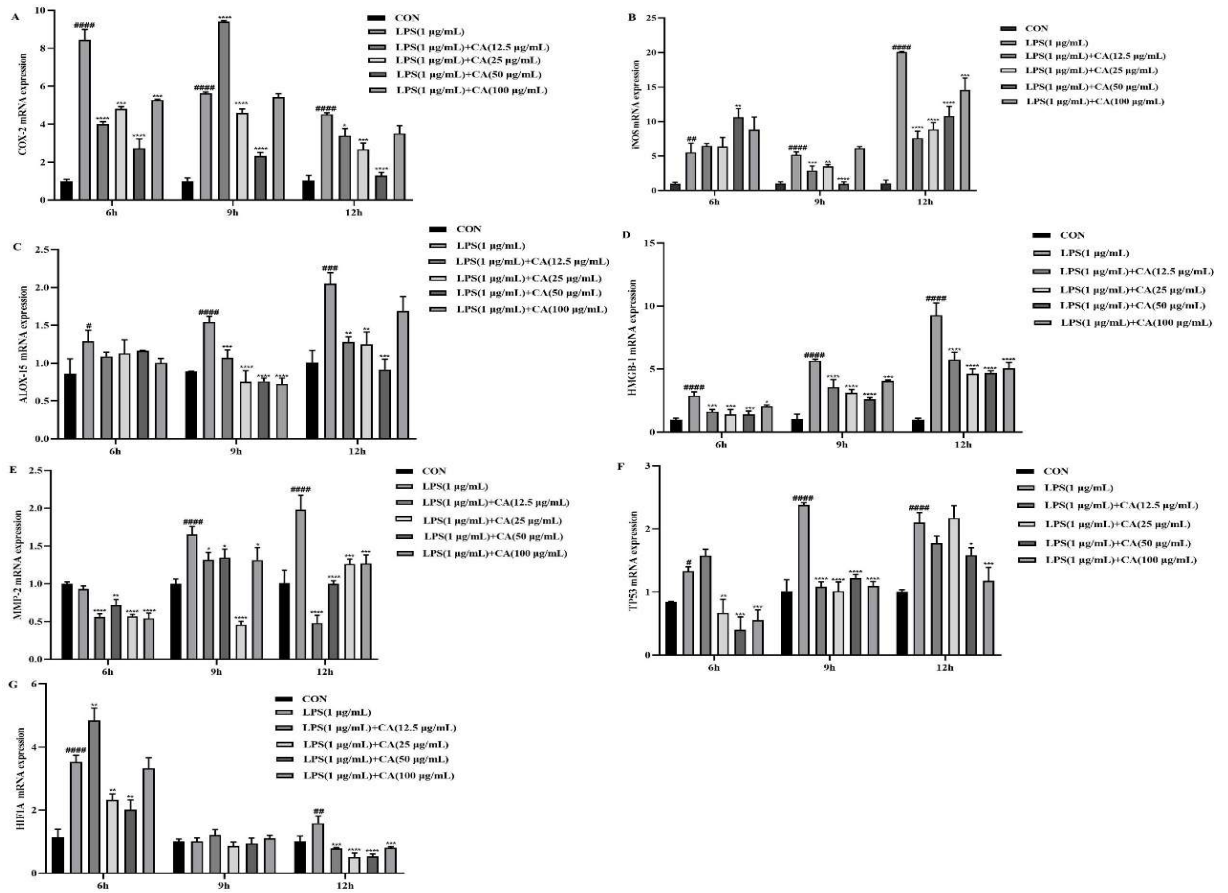

Fig. 6: The effect of CA on LPS-induced inflammatory mediators and HIF-1α/p53 pathway-related mRNA expression in endometrial tissues of dairy cows. The mRNA levels of COX-2 (A), iNOS (B), ALOX-15 (C), HMGB-1 (D), MMP-2 (E), TP53 (F), and HIF-1A (G). * and # denote statistical significance compared to the Con and LPS groups, respectively; *# indicates P<0.05, **## indicates P<0.01, ***### indicates P<0.001, and ****#### indicates P<0.0001.

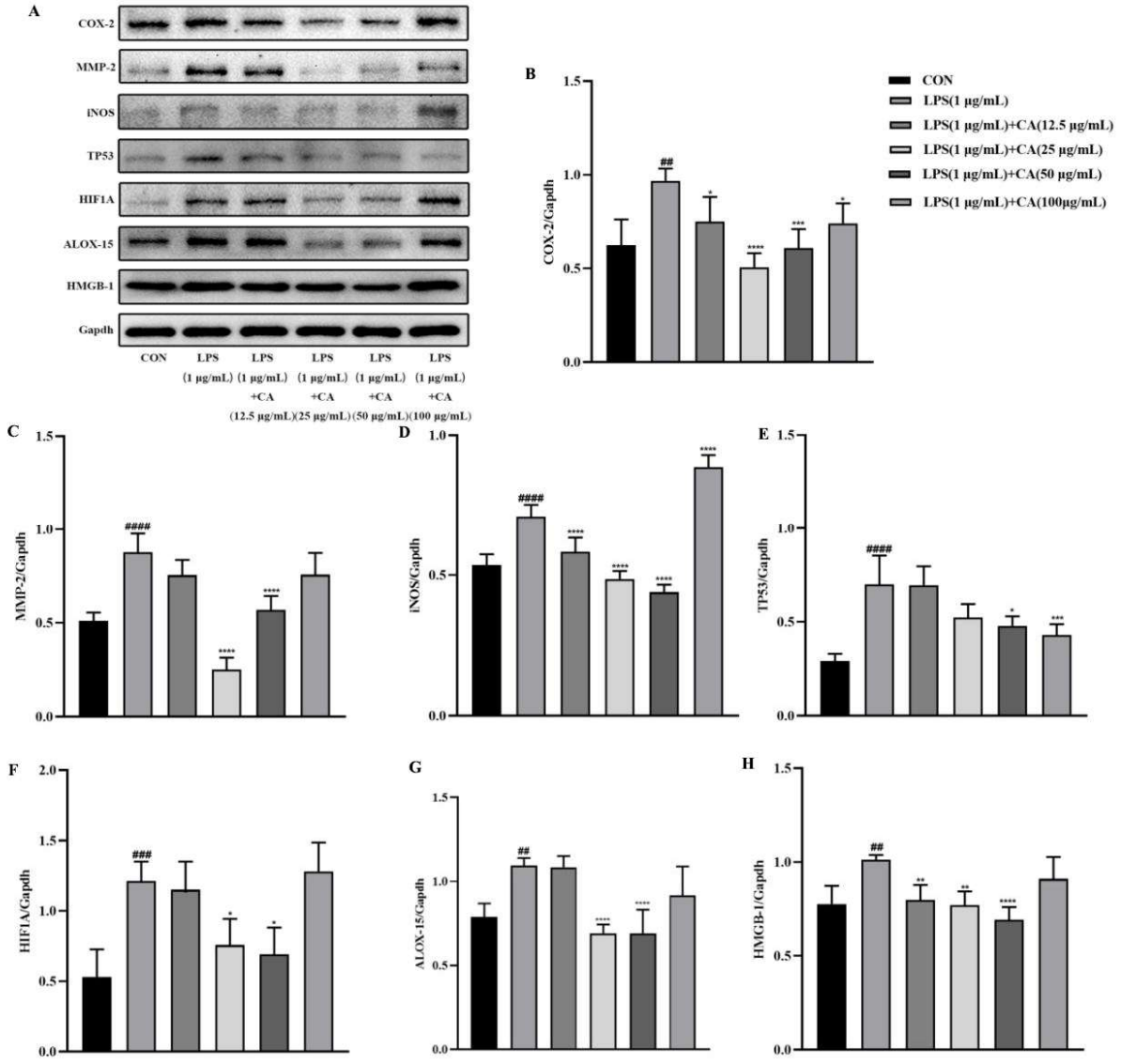

Fig. 7: Chebulagic acid inhibits LPS-mediated increases in the protein expression of inflammatory mediators, TP53, and HIF-1A in the endometrial tissue of dairy cows. (A) Western blot analysis of proteins in CA and LPS-treated endometrial tissue; (B) COX-2; (C) MMP-2; (D) iNOS; (E) TP53; (F) HIF-1A; (G) ALOX-15; (H) HMGB-1. The data were presented as mean ± SD. ##P<0.01, ####P<0.001, #####P<0.0001 vs. Control group, *P<0.05, **P<0.01, ***P<0.001, ****P<0.0001 vs. LPS group.

DISCUSSION

Endometritis is a common postpartum disorder in dairy cattle, primarily caused by bacterial infections. It represents a major cause of infertility, significantly impairing reproductive performance and undermining the economic sustainability of dairy farming (Liu *et al.*, 2021). Current therapeutic options, such as intrauterine antibiotic infusions, are limited by concerns including antibiotic resistance, withdrawal periods, residue contamination, and long-term safety (Zahid *et al.*, 2024). Therefore, identifying novel natural compounds with antibacterial and anti-inflammatory properties holds considerable potential for developing safer and more effective treatments. Escherichia coli is a predominant pathogen associated with bovine endometritis (Wu *et al.*, 2022). This study indicates that CA exerts protective effects in LPS-induced endometritis by downregulating the pro-inflammatory cytokines. The uterus is the primary site of bacterial invasion, and the endometrial epithelium serves as the first barrier to microbial entry (Katila, 2012). Previous studies have shown that CA modulates the production of IL-6, TNF-α, and IL-1β in murine models of LPS-induced inflammation, with results consistent with the present findings (Liu *et al.*, 2025). Additionally, CA treatment reduced the expression levels of other inflammatory mediators (COX-2, iNOS, ALOX-15, MMP-2, and HMGB-1) in LPS-stimulated endometrial tissues. Collectively, these results support the role of CA in mitigating LPS-induced endometritis by suppressing pro-inflammatory signaling pathways.

To elucidate the molecular mechanisms by which CA alleviates endometritis in dairy cows, this study integrated a network pharmacology approach to identify potential therapeutic targets. Analysis revealed that CA interacts with a core set of 16 key molecules (IL-1β, SR2, PPARγ,

ERBB2, BCL2, TGFB1, TP53, SRC, TNF, APP, IGF1R, STAT1, HIF-1α, MMP2, PRKACA, and HDAC1) implicated in inflammatory regulation, cell proliferation, and apoptosis, all central to endometritis pathogenesis. Notably, IL-1β and TNF-α are master regulators of pro-inflammatory signaling, while MMP2 plays a dual functional role: it mediates extracellular matrix (ECM) remodeling and actively modulates inflammation. Dysregulated ECM turnover impairs uterine involution, leading to prolonged recovery and reduced fertility, thereby undermining reproductive efficiency and herd productivity (Tan *et al.*, 2025). The involvement of MMP2 in tissue repair is further supported by evidence from an in vivo mouse model of optic nerve injury, where MMP2 facilitates inflammation-associated axonal regeneration (Andries *et al.*, 2021), underscoring its context-dependent roles in damage response and resolution. In the current study, LPS robustly upregulated both mRNA and protein expression of MMP2 in bovine endometrial tissues. In contrast, CA treatment significantly suppressed MMP2 at both transcriptional and translational levels in LPS-induced endometritis. These molecular findings are strongly corroborated by histopathological assessments using HE staining, which reveal reduced inflammatory infiltration and improved tissue architecture following CA intervention. Collectively, these results provide compelling evidence that CA exerts therapeutic effects against bovine endometritis primarily by coordinating the suppression of inflammatory pathways and restoring tissue homeostasis.

Infections and chronic inflammation are established contributors to carcinogenesis in susceptible tissues, largely through activation of the HIF-1α and p53 signaling pathways. As a master regulator of cellular oxygen sensing, HIF-1α reshapes the endometrial microenvironment by driving the expression of genes critical for angiogenesis and metabolic adaptation. (Corcoran and O'Neill, 2016). Moreover, LPS has been shown to robustly induce p53 upregulation across diverse cell models, including H9c2 cells (Xie *et al.*, 2023), human dental pulp stem cells (Sui *et al.*, 2025), and intestinal epithelial cells (Xie *et al.*, 2019). The present study demonstrates that the HIF-1α/p53 signaling pathway mediates the protective effects of CA against endometritis. LPS induces activation of the HIF-1α/p53 signaling pathway in bovine endometrial tissues, as evidenced by increased expression at both mRNA and protein levels, whereas CA significantly suppresses this activation in a dose-dependent manner. These results provide direct evidence that CA ameliorates endometritis primarily by inhibiting the HIF-1α/p53 signaling axis. These findings further supported transcriptomic and metabolomic profiling, which reveal that inflammatory processes in bovine endometrial epithelial cells are modulated by interconnected regulatory networks involving the TGF-beta signaling pathway, fatty acid metabolism, and p53-associated signaling cascades (Ji *et al.*, 2025).

Conclusions: Our findings indicate that CA ameliorates endometritis primarily by inhibiting the HIF-1α/p53 signaling pathway. These findings elucidate critical molecular mechanisms underlying endometritis in dairy cows and provide a rational basis for developing targeted therapeutic interventions against this inflammatory condition.

Authors contribution: FB, YY, FZ, XR and GZ contributed to investigation, data curation, software and methodology; YY and ZZ performed formal analysis. FB and GZ carried out validation; ZZ and RG led conceptualization and supervision; GZ, RG, HA, EAA and ZZ were responsible for funding acquisition, writing – original draft, review, and editing.

Acknowledgments: This research was funded by Young Talents of Science and Technology in Universities of Inner Mongolia Autonomous Region (NJYT24056), Natural Science Foundation of Inner Mongolia Autonomous Region (2025QN03104 and 2023MS03035), the Special Program for Scientific Innovation Team Construction (Type B Team, BR251303), and the Research Special Project of First Class Discipline by the Education Department of Inner Mongolia Autonomous Region (YLXKZX-NND-012). The authors acknowledge the Princess Nourah bint Abdulrahman University Researchers Supporting Project number (PNURSP2026R460), Princess Nourah bint Abdulrahman University, Riyadh, Saudi Arabia. The authors extend their appreciation to the Deanship of Research and Graduate Studies at King Khalid University for funding this work through the Large Research Project under grant number RGP2/223/46.

REFERENCES

Andries L, Masin L, Salinas-Navarro M, *et al.,* 2021. MMP2 modulates inflammatory response during axonal regeneration in the murine visual system. Cells 10:1672.

Cao L, Liu J, Ye C, *et al.,* 2024. Caffeic acid inhibits *Staphylococcus aureus*-induced endometritis through regulating AMPKα/mTOR/HIF-1α signalling pathway. Journal of Cellular and Molecular Medicine 28:e70175.

Corcoran SE and O'Neill L A 2016. HIF1α and metabolic reprogramming in inflammation. Journal of Clinical Investigation 126:3699-3707.

Ekambaram SP, Aruldhas J, Srinivasan A, *et al.,* 2022. Modulation of NF-κB and MAPK signalling pathways by hydrolysable tannin fraction from *Terminalia chebula* fruits contributes to its anti-inflammatory action in RAW 264.7 cells. Journal of Pharmacuetics and Pharmacology 74:718-729.

Harrach MF and Drossel B, 2014. Structure and dynamics of TIP3P, TIP4P, and TIP5P water near smooth and atomistic walls of different hydroaffinity. Journal of Chemistry and Physics 140:174501.

Heckl M, Schmoeckel E, Hertlein L, *et al.,* 2018. The ARID1A, p53 and ß-Catenin statuses are strong prognosticators in clear cell and endometrioid carcinoma of the ovary and the endometrium. PLoS One 13:e0192881.

Ji G, Feng X, Hu C, *et al.,* 2025. HADHA promotes apoptosis and inflammatory response in bovine endometrial epithelial cells by regulating transcription and metabolism. International Journal of Biology and Macromolecules 304:140980.

Jiang K, Yang J, Xue G, *et al.,* 2021. Fisetin ameliorates the inflammation and oxidative stress in lipopolysaccharide-induced endometritis. Journal of Inflammation Research 14:2963-2978.

Jo S, Kim T, Iyer V G, *et al.,* 2008. CHARMM-GUI: a web-based graphical user interface for CHARMM. Journal of Computational Chemistry 29:1859-1865.

Katila T. 2012. Post-mating inflammatory responses of the uterus. Reproduction in Domestic Animals 47 Suppl 5:31-41.

Kumar N, Gangappa D, Gupta G, *et al.,* 2014. Chebulagic acid from *Terminalia chebula* causes G1 arrest, inhibits NFκB and induces apoptosis in retinoblastoma cells. BMC Complementary and Alternative Medicine 14:319.

Liang D, Qi Y, Liu L, *et al.,* 2023. Jin-Gui-Shen-Qi Wan ameliorates diabetic retinopathy by inhibiting apoptosis of retinal ganglion cells through the Akt/HIF-1α pathway. Chinese Medicine 18:130.

Liu J, Wu Z, Guo S, *et al.,* 2021. IFN-τ attenuates LPS-induced endometritis by restraining HMGB1/NF-κB activation in bEECs. Inflammation 44:1478-1489.

Liu X, Gong Z, Yang Y, *et al.,* 2025. Chebulagic acid inhibits lipopolysaccharide-induced endometritis by regulating mitogen-activated protein kinase/nuclear factor-κB signaling. Journal of Reproductive Immunology 169:104464.

Liu Y, Bao L, Xuan L, *et al.,* 2015. Chebulagic acid inhibits the LPS-induced expression of TNF-α and IL-1β in endothelial cells by suppressing MAPK activation. Experimental and Therapeutic Medicine 10:263-268.

Peng-Fei H, Na A R, Hui C, *et al.,* 2021. Activation of alpha7 nicotinic acetylcholine receptor protects bovine endometrial tissue against LPS-induced inflammatory injury via JAK2/STAT3 pathway and COX-2 derived prostaglandin E(2). European Journal of Pharmacology 900:174067.

Purba FY, Suzuki N and Isobe N, 2021. Association of endometritis and ovarian follicular cyst with mastitis in dairy cows. Journal of Veterinary Medical Science 83:338-343.

Sui Y, Dong X, Tong E, *et al.,* 2025. Artemisinin regulates cell proliferation, apoptosis, and the inflammatory response of human dental pulp stem cells through the p53 signaling pathway under LPS-induced inflammation. International Immunopharmacology 152:114396.

Szklarczyk D, Kirsch R, Koutrouli M, *et al.,* 2023. The STRING database in 2023: protein-protein association networks and functional enrichment analyses for any sequenced genome of interest. Nucleic Acids Research 51:D638-d646.

Tan J, Wang Z, Yang M, *et al.,* 2025. Oxidative stress mediates the dual regulatory effects of bovine uterine ECM remodeling through the TGF-β1/Smad3 pathway: Molecular mechanisms of MMPs and COL-IV imbalances. Animals (Basel) 15(13):1847.

Talib S, Fatima M, Usama M, *et al.,* 2025. Response of single and mixed culture bacteria of *S. aureus* and *E. coli* of camel mastitis against antibiotics and tungsten oxide nanoparticles. Pakistan Journal of Veterinary and Animal Research1(2):34-38.

Wu G, Xu G, Chen D W, *et al.,* 2018. Hypoxia exacerbates inflammatory acute lung injury via the Toll-like receptor 4 signaling pathway. Frontiers of Immunology 9:1667.

Wu J, Bai F, Mao W, *et al.,* 2022. Anti-inflammatory effects of the prostaglandin D(2)/prostaglandin DP1 receptor and lipocalin-type prostaglandin D(2) synthase/prostaglandin D(2) pathways in bacteria-induced bovine endometrial tissue. Veterinary Research 53:98.

Xie MY, Hou LJ, Sun JJ, *et al.,* 2019. Porcine milk exosome MiRNAs attenuate LPS-induced apoptosis through inhibiting TLR4/NF-κB and p53 pathways in intestinal epithelial cells. Journal of Agriculture and Food Chemistry 67:9477-9491.

Xie Z, Yang C and Xu T., 2023. Hesperetin attenuates LPS-induced the inflammatory response and apoptosis of H9c2 by activating the AMPK/P53 signaling pathway. Immunity, Inflammation and Disease 11:e973.

Zahid A, Eiza NU, Khalid M, *et al.,* 2024. Targeting inflammation for the treatment of endometritis in bovines. Microbial Pathogenesis 188:106536.

Zhao L, Zhang J, He J, *et al.,* 2024. Network pharmacology analysis of the regulatory effects and mechanisms of ALAE on sow reproduction *in-vivo* and *in-vitro*. Journal of Ethnopharmacology 334:118525.